Asphalt mixture performance and testing

Precision of complex moduli of asphalt concrete determined by modal analysis

Anders Gudmarsson[1], Jean-Claude Carret[2], Simon Pouget[3], Abubeker Ahmed[4], Richard Nilsson[5], Hervé Di Benedetto[2], Cédric Sauzéat[2]
[1]Peab Asfalt AB, [2]ENTPE, University of Lyon, [3]Eiffage Infrastructures, [4]VTI, [5]Skanska VTC

Abstract

Modal analysis is an economic and repeatable test method to characterize the complex modulus of asphalt concrete specimens. The method have shown good agreement to conventional tension-compression cyclic loading and to non-destructive in-situ stiffness measurements of pavements. The testing is performed by applying impacts to a specimen using a small hammer. The frequency content of the input load and the frequency response of the specimen are measured to determine the complex modulus. This paper presents an evaluation of the complex modulus reproducibility by performing modal analysis on asphalt concrete specimens at several laboratories. The testing is repeated at a number of temperatures to evaluate the precision of the method over a wide range of the frequency and temperature dependent master curve. The simple practical test set-up and truly non-destructive nature of the modal analysis testing are some of the advantages that contribute to the good precision of the complex modulus characterization of asphalt concrete. In addition, practical aspects that are of importance for accurate testing are highlighted.

This paper was first published in 2020 in version 1.0 of the proceedings of the 7th E&E Congress. This second edition (version 1.1.) of the proceedings is published in June 2021. The content of this paper has not changed, but the author(s) may have provided additional information in the form of an annex.

1. INTRODUCTION

The complex moduli is a key parameter to characterize the linear viscoelasticity of asphalt concrete. The viscoelastic properties governs the mechanical performance and the dynamic moduli, defined as the absolute value of the complex moduli, is used in thickness design of pavements [1, 2]. Conventional test methods to determine the complex moduli of asphalt concrete applies stresses to specimens through cyclic loading and measures the resulting strains [2, 3]. The complex moduli master curve is determined by repeating the measurements at several temperatures and loading frequencies (e.g. -20 to 50 °C and 0.01 to 25 Hz). It is well recognized that conventional complex moduli testing is expensive due to the equipment costs and the time consuming measurements [4].

Modal analysis is a widely used methodology to characterize the dynamic properties of solids in several fields of engineering [5]. The principle of the testing is to determine frequency response functions (FRFs) by exciting the natural frequencies of a solid or a system. A FRF describe the response to an applied force as a function of frequency and is determined from measuring the input load and the response of the solid (displacement, velocity or acceleration at specific points). The measured FRFs are used to characterize material properties by curve fitting of FRFs calculated by an analytical or numerical model. In recent years, modal analysis has also been applied to characterize the complex moduli of asphalt concrete cf. e.g. [6-9]. Distinctive of modal analysis applied to asphalt concrete is that the complex moduli are determined at smaller strain levels and at higher loading frequencies in comparison to conventional cyclic loading. Since modal analysis has proven to be a simple, economic and accurate test method, it holds a great potential to complement conventional cyclic testing to characterize asphalt concrete at higher loading frequencies and smaller strain levels. Furthermore, to determine the complex moduli master curve, the testing is repeated only at different temperatures since a single measurement covers a wide frequency range, which depend on the stiffness (e.g. 5 to 20 kHz).

Previous studies show that the complex moduli determined from modal analysis are in good agreement to cyclic tension-compression testing [8, 10, 11], and modal analysis applied to cylindrical specimens results in a good reproducibility of the complex moduli [12]. In addition, modal analysis provides a link to surface wave measurements for non-destructive quality control of pavements [13]. In this paper, the reproducibility of modal analysis to beam shaped asphalt concrete specimens are evaluated. In addition, practical aspects of using an impact hammer and the test set-up that are important for accurate testing are highlighted.

2. METHODOLOGY

2.1. Experimental measurements

Modal analysis was performed to two beam shaped asphalt concrete specimens at five laboratories (see specimen specifications in Table 1). The specimens were sawn from slabs compacted in a laboratory and the mix had a gap-graded curve with 30 % recycled asphalt and 4.7 % polymer modified bitumen. The testing was performed by applying an impact load to excite the longitudinal modes of vibration and measuring the responding free vibrations in terms of acceleration. The laboratories used the same type of impact hammer to apply the load and similar type of accelerometers. The impacts and the accelerometers were applied to the same positions on the specimens at each laboratory. Automated or manual hammer impacts were applied depending on the laboratory performing the testing [8]. In all cases, the accelerometers were glued to the specimens, which were placed on soft foam and conditioned in a temperature chamber between 4 to 6 hours. The testing temperatures were approximately -20, 0, 15, 35 and 50 °C. The testing was performed inside a closed chamber, with an open chamber door, or completely outside of the chamber depending on the choice of the laboratory.

Table 1. Specifications of the specimens

Specimen	Length (mm)	Width (mm)	Height (mm)	Density (kg/m³)	Air voids (%)
B2	299.8	50.3	50.2	2399	3.3
B4	300.0	50.4	49.8	2409	2.9

The set-up of the equipment is shown in Figure 1 where the impact hammer and accelerometer are connected via a signal conditioner to a data acquisition (DAQ) device. The measurements are controlled and processed through a computer using a software application developed in MATLAB [14].

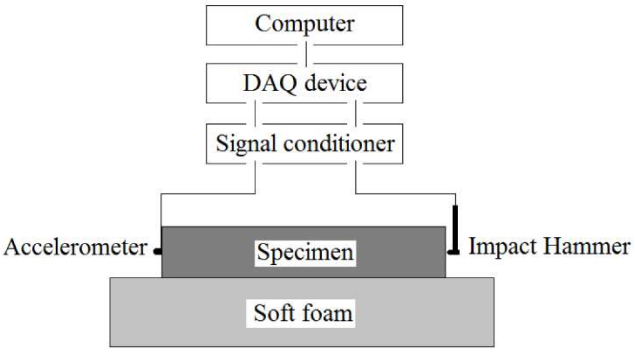

Figure 1: Test set-up of modal analysis [6]

The same type of equipment and test set-up were used by the laboratories to perform the measurements. The following equipment models were used to measure the FRFs:

- Impact hammer (PCB model 086E80)
- Accelerometer (PCB model 352B10 and PCB model 353B15)
- Signal conditioner (PCB model 480B21 and PCB model 482C15)
- Data acquisition device (NI USB-6251 M series, NI USB-6356 X series and NI USB-4432)
- Computer

The frequency response functions (FRFs) are determined from the Fourier transform of the measured input load and response of the specimen by calculating the ratio of the complex valued cross-spectrum (input and output) to the complex valued power spectrum (input) according to Equation 1.

$$H(f) = \big(Y(f) \cdot X^*(f)\big) / \big(X(f) \cdot X^*(f)\big) \quad (1)$$

where $H(f)$ is the complex frequency response function, $Y(f)$ is the measured acceleration, $X(f)$ is the measured input force and $X^*(f)$ is the complex conjugate of the input force. Five measurements of the impact force and response were used to determine an average of the complex FRFs for each specimen and measurement temperature. The absolute value of the averaged complex FRFs were further used to characterize the complex moduli.

2.2. Characterizing the complex moduli

The complex moduli were determined by matching numerically computed FRFs to the measured FRFs. The FRFs were computed by using the finite element method and performing a frequency domain study in the three-dimensional space assuming homogenous and isotropic material properties (complex modulus, E^* and complex Poisson's ratio, ν^*) [6]. A 1 N point load was defined according to the position of the hammer impact to compute the longitudinal modes of vibration. The acceleration was determined in the position according to the accelerometer placement. The optimization of the FRFs to the measurements were performed by using MATLAB or a software application developed in COMSOL Multiphysics Application Builder [6, 12, 14].

The linear viscoelastic material properties were expressed by either the Havriliak-Negami (HN) model [15] or the 2S2P1D model [4]. Each laboratory decided which model to use. The complex moduli are presented in equation 2 and 3 for the HN and the 2S2P1D model, respectively.

$$E^*_{HN}(\omega) = E_\infty + \frac{E_0 - E_\infty}{(1+(i\omega\tau)^\alpha)^\beta} \quad (2)$$

where E_0 is the low frequency value of the modulus. E_∞ is the high frequency value of the modulus. ω is the angular frequency ($\omega = 2\pi f$, f is the frequency), α governs the width of the loss factor peak, β governs the asymmetry of the loss factor peak, $\tau = 1/\omega_0$ is the relaxation time, which describes the position of the loss factor peak along the frequency axis and where ω_0 is the frequency at the loss factor peak.

$$E^*_{2S2P1D}(\omega) = E_{00} + \frac{E_0 - E_{00}}{1+\delta(i\omega\tau)^{-k}+(i\omega\tau)^{-h}+(i\omega\beta\tau)^{-1}} \quad (3)$$

where E_{00} is the low frequency value of the modulus. E_0 is the high frequency value of the modulus. δ is a constant, k and h are exponents according to $0<k<h<1$, β is a dimensionless constant related to the Newtonian viscosity (η) according to $\eta = (E_0 - E_{00})\,\beta\tau$, and τ is characteristic time depending only on the temperature.

The HN and 2S2P1D models were used to characterize the complex Poisson's ratio (ν^*) correspondingly to Equation 2 and 3 of the complex moduli [12]. The parameters of the HN and 2S2P1D models were estimated through the optimization of the computed FRF to the measured FRFs at each test temperature. The low frequency parameters of the HN (E_0 = 100 MPa and ν_0 = 0.5) and the 2S2P1D (E_{00} = 100 MPa, ν_{00} = 0.5, h = 0.53 and β = 250) model were assumed since realistic values corresponding to the material properties of asphalt concrete does not affect the computed FRFs.

The Williams-Landel-Ferry (WLF) shift factor equation [16] was used to shift the characterized complex modulus according to the time-temperature superposition principle [17] and to determine the complex moduli master curves.

$$\log \alpha_T(T) = \frac{-c_1(T-T_{ref})}{c_2+T-T_{ref}} \quad (4)$$

where T is the test temperature, and c_1 and c_2 are material constants at the reference temperature (T_{ref}).

3. RESULTS

3.1. Position of the hammer impact

Four hammer impacts where applied to an asphalt concrete specimen at 20 °C to demonstrate that the positioning of the impact influences the frequency range used to characterize the complex moduli. Two impacts were applied to a stone and two impacts were applied to the bitumen (or mastic). In addition, impact number one to the stone was applied with a larger force compared to impact number two to the stone. Figure 2 illustrates the different hammer positions of the impacts, where Figure 2*a* shows the position of the bitumen impact and Figure 2*b* shows the position of the stone impact.

(*a*)  (*b*) 

Figure 2: Illustration of an impact to bitumen (*a*) and an impact to a stone (*b*)

Because a shorter duration of the load pulse excites a wider frequency range, it is beneficial to apply the hammer impacts to a stone. This is shown in Figure 3 by comparing the impacts to the stone (1 and 2) to the impacts to the bitumen (3 and 4). The impacts to the stone results in a duration of the load pulse of approximately 0.05 ms and the impacts to the bitumen gives a duration of approximately 0.1 ms (see Figure 3*a*). Figure 3*b* shows the effect of the four impacts in frequency domain and highlights the differences in magnitude of the force with increasing frequencies. While the shorter load pulse duration of the stone impacts contains energy and excites frequencies up to at least 30 kHz, the impact to the bitumen does not provide so much energy at frequencies above approximately 15 kHz. This shows that the characterization of the complex moduli based on the bitumen impacts may be limited to below 15 kHz. The duration of the load pulse from impacts applied to bitumen is also depending on the bitumen stiffness (bitumen type and test temperature). Therefore, applying impacts to the bitumen instead of stones may result in a larger variation of the frequency range that can be excited in the modal testing.

Figure 4 show the measured response of the specimen by the acceleration in time (4*a*) and frequency (4*b*) domain. In comparison to the impacts to the stone, it is obvious also in this figure that the impacts to the bitumen excites the higher resonance frequencies with a much smaller level of energy.

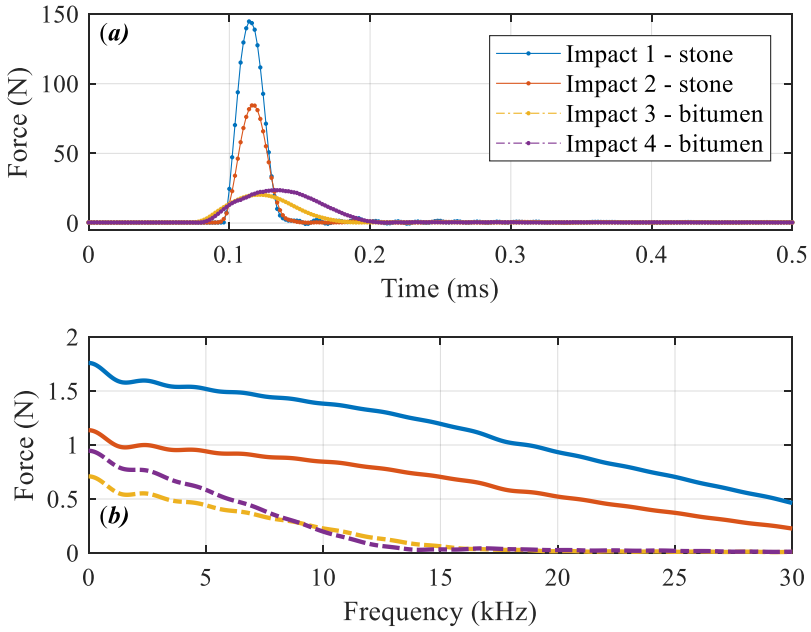

Figure 3: Force in time (*a*) and frequency (*b*) domain of hammer impacts to stone and bitumen

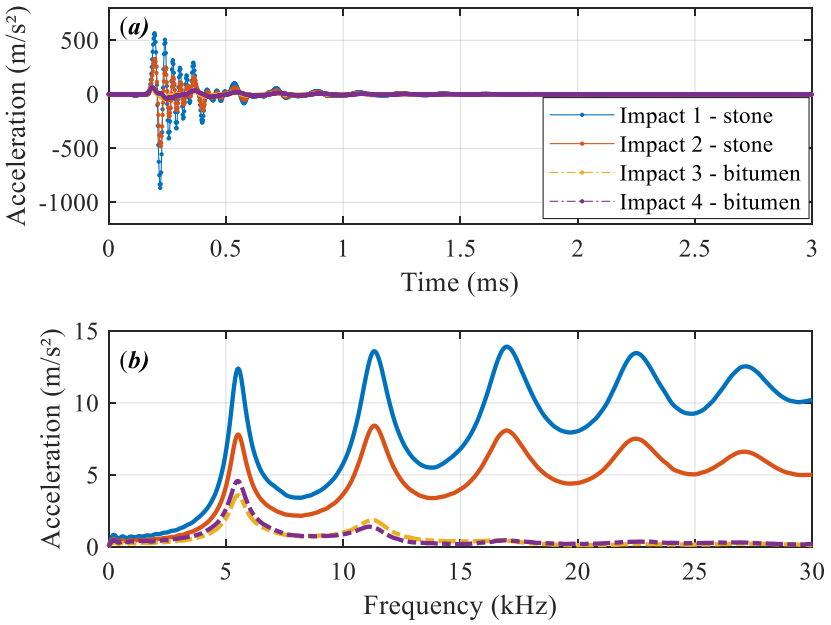

Figure 4: Responding acceleration in time (*a*) and frequency (*b*) domain due to hammer impacts to stone and bitumen

Figure 5 presents the absolute value of the complex FRFs. This figure shows that the FRFs of the bitumen impacts are becoming noisy at frequencies from approximately 12 kHz and above due to the low energy at higher frequencies. On the other hand, the different force applied in the two impacts to the stone does not have an influence on the resulting FRFs, which is also shown in Figure 5. The averaged complex FRF, calculated from the mean of the cross-spectrum and the mean of the power spectrum, reduces the impact of FRFs with noise relatively large to the input and output signals. Figure 5 shows that the absolute value of the averaged complex FRF of the four measurements follows the FRFs of the impacts to the stone with less noise relatively to the input and output signals.

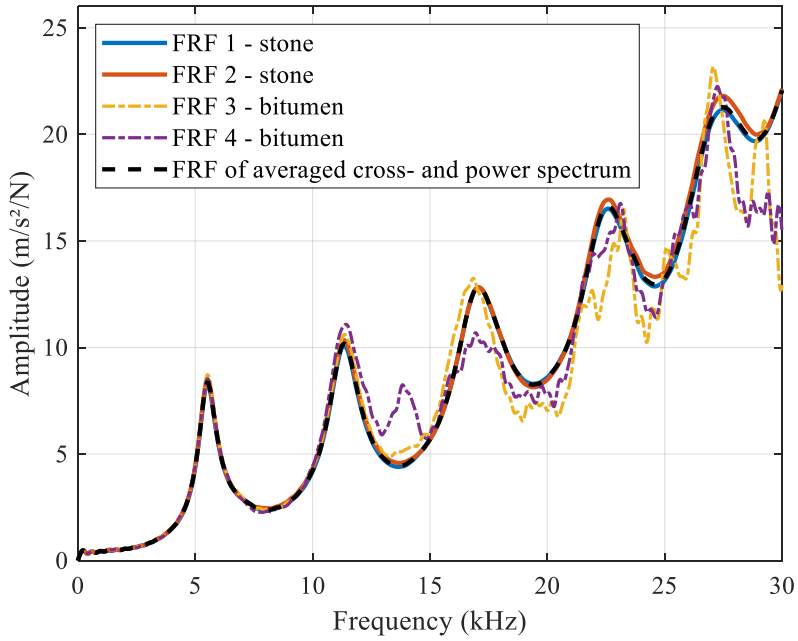

Figure 5: Absolute value of the complex FRFs determined from impacts to stone and bitumen and the complex FRF of the averaged cross- and power spectrum

3.2. Influence of the test system

The test equipment may cause disturbances to the measurements if the connected system is not given time to be stabilized before the testing is performed. Testing immediately after either powering up the devices or connecting the cables are possible sources for disturbance to the measurements. Figure 6 shows two sets of measurements presented in time domain as an example of the effect of a stabilized and non-stabilized test system. In the case of the non-stabilized system, the accelerometer was connected to the already powered signal conditioner just before the testing were performed. The signal of the accelerometer was therefore not stabilized which results in that the amplitude does not start at zero (see Figure 6). Furthermore, five repeated impacts results in five response signals with five different amplitudes. Hence, the amplitude of the accelerometer signal has been affected by the fact that the system is not stabilized. Figure 6 also shows that the amplitudes of measurements performed with a stabilized system starts at zero for all five signals. Note that a pre-trigger time is defined, which means that the recording starts 0.1 ms before the specimens are excited by the impact.

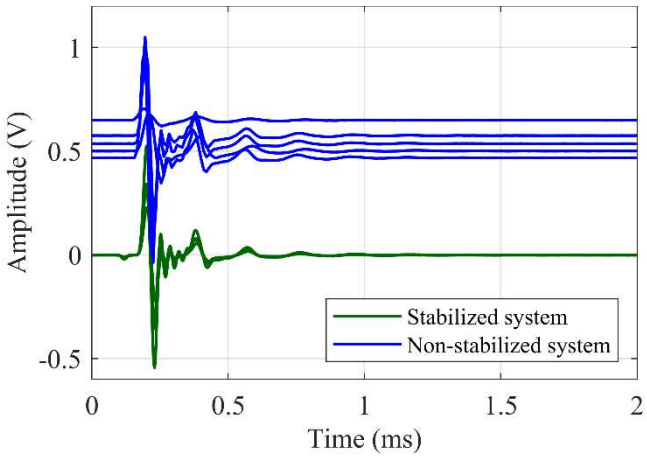

Figure 6: Response signals of measurements with a stabilized and non-stabilized system.

The FRF of the non-stabilized test set-up shows a clear difference in amplitude to FRFs measured with a stabilized system. Figure 7 shows five FRFs of specimen B2 at approximately 0 °C, where FRF labelled E was measured by a non-stabilized system due to the late accelerometer connection as described above. The amplitude of this FRF (E)

is higher compared to the other FRFs (A to D), which were measured by a stabilized system (zero amplitude of the response signals at time zero).

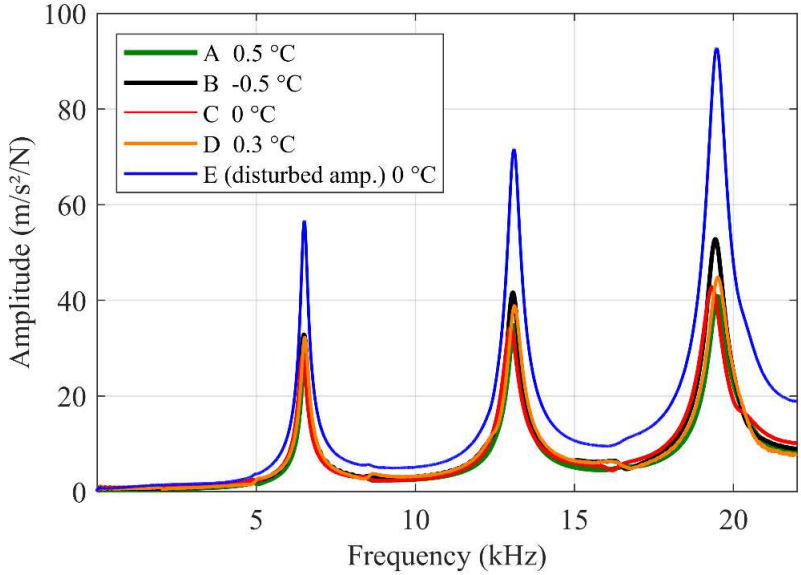

Figure 7: Absolute value of the FRFs of specimen B2 at 0 °C showing a FRF disturbed by the testing equipment

3.3. Precision of modal analysis to beam shaped specimens

The testing of the beam shaped specimens at the five laboratories resulted in similar resonance frequencies of the FRFs. The amplitudes of the FRFs resulted in higher coefficient of variation (CV) in comparison to the resonance frequencies at all testing temperatures. These results are in agreement with the testing performed on cylindrical specimens at different laboratories [12]. The resonance frequencies mainly depend on the elastic storage modulus and the viscous loss modulus affect the amplitude of the FRFs.

The FRFs determined from testing of specimen B2 at 0 °C are presented in Figure 8. The three first resonance frequencies of the FRFs measured at the five laboratories are between 6.46 and 6.53 kHz (CV = 0.43 %), 12.9 and 13.1 kHz (CV = 0.43 %), and between 19.3 and 19.5 kHz (CV = 0.42 %), respectively. The peak amplitudes of the FRFs at the resonance frequencies also show a good reproducibility but with higher CV, 6.1 %, 8.1 % and 10.4 %, respectively. Note that the measurements are not expected to results in the exact same FRFs due to the small differences in testing temperatures between the laboratories. The differences in temperatures are accounted for in the determination of the complex moduli master curves.

The variations in amplitude between the FRFs have a smaller contribution to the complex modulus at lower temperatures and higher frequencies where the loss modulus is relatively small to the storage modulus. However, as the storage modulus decreases with higher temperatures and lower frequencies, the loss modulus contribution to the complex modulus increases. This means that the variations in amplitudes of the FRFs becomes more significant to the variations of the complex moduli with increasing temperatures.

Figure 9 presents the complex moduli master curves from the five laboratories determined for specimen B2 over the frequency range of 10^{-1} to 10^{11} Hz and at a reference temperature of 15 °C. The dynamic modulus master curve (see Figure 9*a*) indicate a good agreement of the different laboratories. Note that one laboratory applied the 2S2P1D model and the others applied the HN model to characterize the complex moduli. Figure 9*b*, showing the phase angle, indicate an increasing variation between the laboratories with decreasing frequencies. Furthermore, the Cole-Cole diagram in Figure 9*c* show that the variation of the phase angle can be explained by the differences of the characterized loss moduli. The increasing impact of the loss modulus increases the variation to the complex moduli at lower stiffness of the asphalt concrete. Table 2 presents the CV of the dynamic modulus and the standard deviation (SD) of the phase angle for the two specimens. The dynamic moduli and the phase angle characterized by the modal analysis results in a very good reproducibility, especially for frequencies of 10 Hz and above, while the lower frequency range below 10 Hz results in higher values of the CV and SD. In general, the values of the CV over the wide frequency range are low compared to other complex modulus test methods of asphalt [18, 19, 20] and bitumen [21, 22].

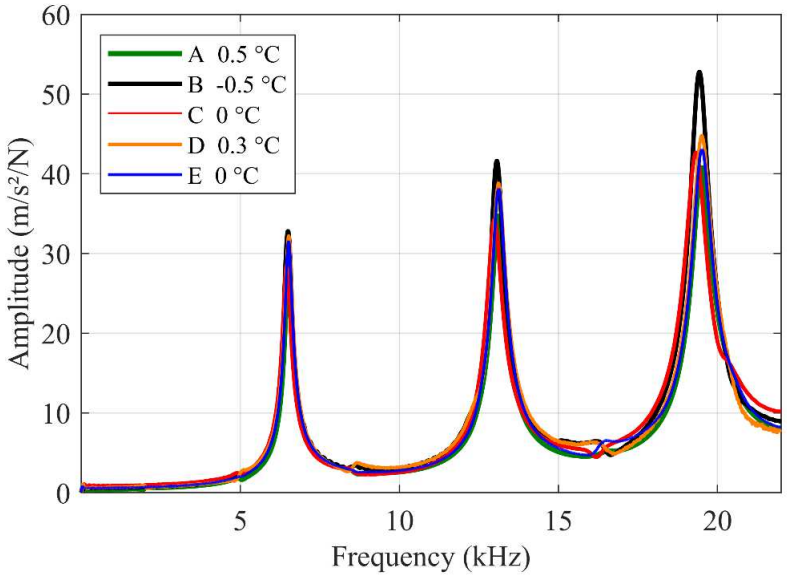

Figure 8: Absolute value of the FRFs of specimen B2 at 0 °C

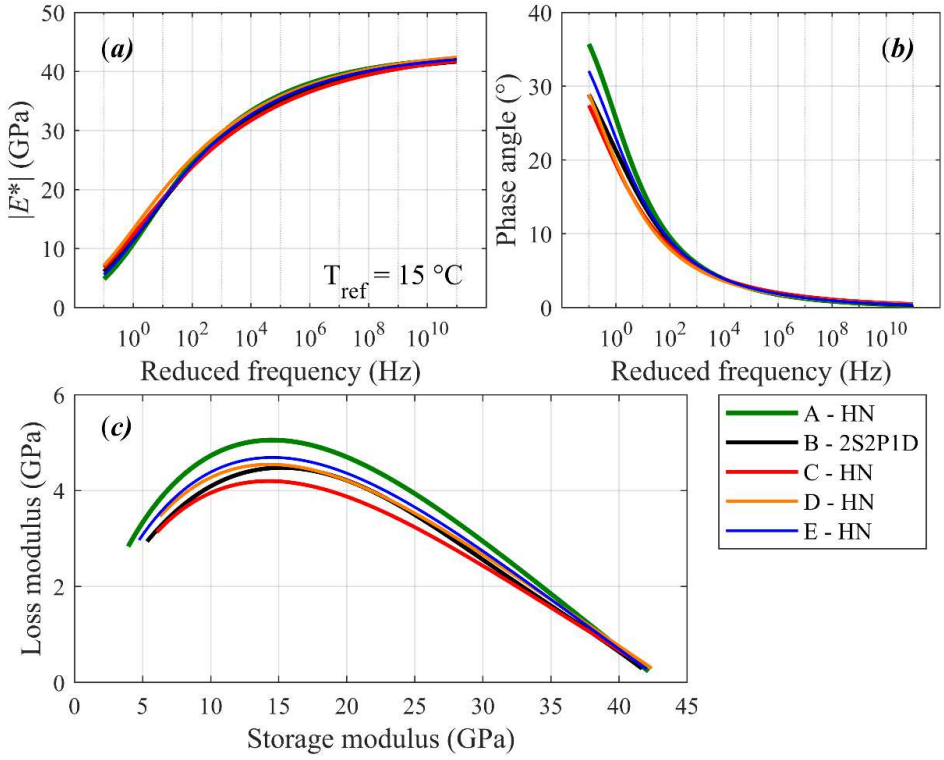

Figure 9: Complex modulus master curves of specimen B2

Table 2. CV of the dynamic modulus and SD of the phase angle

Specimen	Frequency range (Hz)	Max CV (%)	Min CV (%)	Max SD (°)	Min SD (°)
B2	0.1 to 10	15.2	3.9	3.3	1.4
	10 to 10^{11}	3.9	0.7	1.4	0.06
B4	0.1 to 10	14.6	3.3	3.6	1.2
	10 to 10^{11}	3.3	1.2	1.2	0.07

4. CONCLUSIONS

The modal analysis performed at five laboratories to two beam shaped asphalt concrete specimens resulted in dynamic moduli master curves with values of the CV below 4 % for loading frequencies above 10 Hz. At lower frequencies, the CV increases due to an increased impact of the differences in the amplitudes of the FRFs. The results show that modal analysis applied to asphalt concrete contribute to an improved precision of the characterization of the complex moduli.

Care should be taken to the positioning of the input load when using an impact hammer to excite the specimens. Impacts generating a short duration of the load pulse results in that FRFs can be determined over a wider frequency range with less noise. In practice, this can be achieved by applying the impacts to a stone. FRFs measured over a wide frequency range improves the accuracy of the characterization of the complex moduli. The set-up of the test equipment and controlling the status of the system before testing are also important factors to perform accurate measurements.

ACKNOWLEDGEMENTS

The Swedish Transport Administration and the Development Fund of the Swedish Construction Industry (SBUF) are gratefully acknowledged for the financial support. Members of the reference group including Kenneth Lind, Lars Jansson, Jonas Ekblad, Bernardita Lira, Mats Wendel, Nils Rydén, Silvana Torres and Laio Guimaraes-Oliveira are also acknowledged for their contribution to this project.

REFERENCES

[1] Nazarian, S., Yuan, D., Tandon, V., Structural Field Testing of Flexible Pavement Layers with Seismic Methods for Quality Control, J. Transp. Res. Board, 1654, 1999, 50-60, https://doi.org/10.3141/1654-06
[2] Di Benedetto, H., Delaporte, B., Sauzéat, C., Three-Dimensional Linear Behavior of Bituminous Materials: Experiments and Modeling, Int. J. Geomech., Vol. 7, No. 2, 2007, 149-157
[3] Daniel, J., Chehab, G., Kim, Y. R., Issues Affecting Measurement of the Complex Modulus of Asphalt Concrete, J. Mater. Civ. Eng. 16, Special Issue: Strengthening of Concrete Structures with Advanced Composite Materials-Prospects and Problems, 2004, 469–476
[4] Olard, F., Di Benedetto, H., General “2S2P1D” Model and Relation Between the Linear Viscoelastic Behaviours of Bituminous Binders and Mixes, Road Mater. Pavement, Vol. 4, No. 2, 2003, 185-224.
[5] Halvorsen, W. G., Brown, D., L., Impulse Technique for Structural Frequency Response Testing, Journal of Sound and Vibration, 1977, 8-21
[6] Gudmarsson, A., Ryden, N., Birgisson, B., Characterizing the low strain complex modulus of asphalt concrete specimens through optimization of frequency response functions, J. Acoust. Soc. Am., Vol. 132, Issue 4, 2012, pp. 2304-2312
[7] Gudmarsson, A., Ryden, N., Birgisson, B., Observed deviations from isotropic linear viscoelastic behaviour of asphalt concrete through modal testing, Construction and Building Materials, Vol. 66, 2014, 63-71
[8] Carret, J-C., Pedraza, A, Di Benedetto, H, Sauzéat, C., Comparison of the 3-dim linear viscoelastic behavior of asphalt mixes determined with tension-compression and dynamic tests, Construction and Building Materials, Vol. 174, 2018, 529-536
[9] Barriera, M., Lebental, B., Pouget, S., Towards road pavement response under moving loads, Road Materials and Pavement Design, 20:sup1, 2019, S480-S499, DOI: 10.1080/14680629.2019.1588780
[10] Gudmarsson, A., Ryden, N., Di Benedetto, H., Sauzéat, C., Tapsoba, N., Birgisson, B., Comparing linear viscoelastic properties of asphalt concrete measured by laboratory seismic and tension-compression tests, Journal of Nondestructive Evaluation, Vol. 33, Issue 4, 2014, 571-582
[11] Gudmarsson, A., Ryden, N., Di Benedetto, H., Sauzéat, C., Complex modulus and complex Poisson’s ratio from cyclic and dynamic modal testing of asphalt concrete, Construction and Building Materials, Vol. 88, 2015, pp. 20-31
[12] Gudmarsson, A., Carret, J-C., Pouget, S., Nilsson, R., Ahmed, A., Di Benedetto, H., Sauzéat, C., Precision of modal analysis to characterise the complex modulus of asphalt concrete, Road Materials and Pavement Design, 20:sup1, 2019, S217-S232, DOI: 10.1080/14680629.2019.1590224
[13] Bjurström, H., Gudmarsson, A., Ryden, N., Starkhammar, J.. Field and laboratory stress-wave measurements of asphalt concrete, Construction and Building Materials, Vol. 126, 2016, pp. 508-516
[14] Gudmarsson, A., and Ryden, N., Apps for modal analysis to characterize the complex modulus of asphalt concrete, Bearing Capacity of Roads, Railways and Airfields – Loizos et al. (Eds), 201,7 pp. 209-215, Taylor & Francis Group, London, ISBN 978-1-138-29595-7

[15] Havriliak, S., and Negami, S., A complex plane analysis of α-dispersions in some polymer systems, J. Polym. Sci. C, Vol. 14, 1966, 99–117
[16] Williams, M. L., Landel, R. F., Ferry, J. D, The temperature dependence of relaxation mechanisms in amorphous polymers and other glass-forming liquids, J. Am. Chem. Soc., Vol. 77, 1955
[17] Nguyen, H. M., Pouget, S., Di Benedetto, H., Sauzéat, C., Time-temperature superposition principle for bituminous mixtures, European Journal of Environmental and Civil Engineering, 13:9, 2009, 1095-1107, DOI: 10.1080/19648189.2009.9693176
[18] Dougan, C.E., Stephens, J.E., Mahoney, J., Hansen, G.: E∗—Dynamic Modulus. Test Protocol—Problems and Solutions. University of Connecticut, Storrs, CT-SPR-0003084-F-03-3, 2003
[19] Bennert, T., Dynamic modulus of hot mix asphalt (Final Report FHWA-NJ-2009-011). Trenton, New Jersey: New Jersey Department of Transportation, 2009
[20] Hakim, H., Nilsson, R., Vieira, J. M., Said, S., Round robin test of stiffness modulus by indirect tensile method according to EN 12697-26:2004 ANNEX C, 5th Eurasphalt & Eurobitume Congress, Istanbul, Turkey, 13-15th June 2012
[21] Eckmann, B., Largeaud, S., et al., Measuring the rheological properties of bituminous binders final results from the round robin test of the BNPÉ/P04/GE1 Working Group (France). 5th Eurasphalt & Eurobitume Congress, Istanbul, Turkey, 13-15th June 2012
[22] Sybilski D., Vanelstraete A., Precision of bituminous binder rheology tests in the 2nd Rilem round robin test, 6th Rilem symposium PTEBM'03, 2003, Zurich